Sensors & Transducers, Vol. 27, Special Issue, May 2014, pp. 106-115

Sensors & Transducers

http://www.sensorsportal.com

In situ Sensitivity Improvement of NMR Receiver Probes (Coils and Microcoils)

[1, 2] Josué TREJO ROSILLO, [2] Youssef Zaim WADGHIRI, [1] Latifa Fakri-BOUCHET

[1] Université de Lyon, CREATIS; CNRS UMR 5220; INSERM U1044; INSA-Lyon, Université Lyon 1; 69622 Villeurbanne, France
[2] New York University, Medical Center; New York, USA
Tel.: (+33) 4 72 43 19 25, fax: (+33) 4 72 44 81 99
E-mail: latifa.fakri-bouchet@ creatis.insa-lyon.fr

Received: 31 December 2012 /Accepted: 10 August 2013 /Published: 26 May 2014

Abstract: The sensitivity is a main problem for NMR experiments and it is laid down by the thermal noise of the receiver coil and its geometry. To improve the sensitivity of an NMR receiver coil, considering the postulate of Friis, the signal must be amplified as close as possible to the coil. Here we present a method to achieve optimum in situ low noise amplification for the sensitivity improvement of an NMR receiver coil or microcoil. In this paper we propose a realistic transducer model of an NMR coil and a reliable method to model an LNA. We introduce the requirements to achieve a low noise matching network for NMR receivers allowing an improvement of the sensitivity of the coil by a factor of 6. This sensitivity improvement has its interest in MRI by increasing the field of view with a higher SNR but also in MRS by reducing the limit of detection. *Copyright © 2014 IFSA Publishing, S. L.*

Keywords: Nuclear Magnetic Resonance, Transducer NMR receiver coil model, SNR, Noise matching, LNA model, NMR sensitivity improvement.

1. Introduction

The Nuclear Magnetic Resonance Spectroscopy (MRS), one of the most common analysis methods used in biochemistry over more than twenty years [1–3], allows getting very precise information about a sample even for pico-metric volume scales [4, 5]. In this case, the signal to noise ratio (SNR) is improved when the NMR receiver coil is as close as possible to the sample, the NMR coil matching the sample size [4–6].

A chronically implantable receiver microcoil has been developed in previous works [7–11] for following cerebral metabolites variations in the Alzheimer Disease animal model by localized MRS. This microcoil is a 1000 µm * 500 µm ellipsoidal surface coil with 4 turns fabricated by electrolytic deposition of 38 µm of copper on a glass substrate (Fig. 1). NMR in vitro measurements of ^{1}H, under a static magnetic field of 4.7 T (work frequency: 200 MHz), were achieved with this microcoil; its active observation volume is 2 µl. Moreover, a biocompatibility study showed that this microcoil can reach its aim: be implanted in order to measure the rodent cerebral metabolites. However, the concentration limit of detection (LODc) is about 5 %; this means that the sensitivity of the coil is very weak: concentration sensitivity ≈ 0.3 [8].

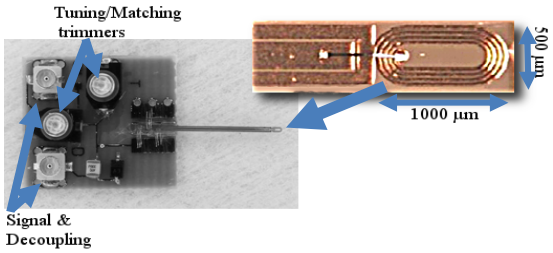

Fig. 1. Micro-coil and tuning/matching PCB.

The microcoil low sensitivity is due to noise induced by the coaxial cables [12], PCBs, connectors and lumped element losses of the data acquisition line. Moreover, the absence of isolation between the micrometric coil and the matching circuit (centimetric PCB) and the coaxial cables (metric) can induce signal losses [13].

A solution to isolate an NMR surface coil from the data acquisition line consist to amplify the signal between them but most of the actual developments dealing with NMR amplification still uses a coaxial cable between the coil and the amplifier [14, 15].

We propose here a methodology to associate a Low Noise Amplifier (LNA) as close as possible to the coil [16, 17] by using an optimized matching network in a single PCB. This solution allows enhancing the SNR and then the coil sensitivity: the objective of this study.

In the paragraph 2, we will define the sensitivity of an NMR coil and its relationship with the low noise signal amplification. In this context, we will introduce the matching network requirements for NMR receiver coils. In paragraph 3, the models of the surface coil and the LNA will be presented as well as the optimum matching network and the simulation results. In the paragraph 4, we will present the test bench circuit verification and the validation of our method in an NMR system.

2. Theory

It is important to state that this is a preliminary study so the first developments were performed with a surface coil of 1.5 cm of radius, and should be extrapolated to the microcoil. The aim of this work is to demonstrate the benefits of local low noise amplification, the considerations to achieve it and finally the potential future applications.

2.1. Sensitivity of an NMR Receiver Coil and Local Low Noise Amplification

The sensitivity of an NMR receiver coil termed by the concentration sensitivity is expressed as the ratio between the signal to noise ratio (SNR) and the concentration of the measured substance [18]:

$$S_c = \frac{SNR}{concentration}, \quad (1)$$

In NMR, the signal to noise ratio is given by [19], [20]:

$$SNR = \frac{\mu(signalpower)}{\sigma(noisepower)},$$

$$SNR \propto \omega_0 B_0 V_S \frac{B_1}{i} \frac{1}{\sqrt{4k_B T_S R_S \Delta f}}, \quad (2)$$

where k_B is the Boltzmann constant, T_S and R_s are the ambient temperature and the source resistance respectively (here the source is the coil) and Δf is the receiver bandwidth.

In this expression we can state two main components, the components depending on the environment and the geometrical components:

The environment components are the static magnetic field (B_0), the Larmor precession frequency proportional to B_0 (ω_0) and the sample volume (V_s).

The geometrical components are B_1/i which is equivalent to the NMR signal and $\sqrt{4k_B T_s R_s \Delta f}$ which represents the noise produced by the coil in a given bandwidth [21].

As we can see, the environment components are constants imposed by the work conditions, and, if the geometrical parameters are optimized to achieved a maximum B_1/i and a low noise (minimum R_s), the only solution to improve the SNR is to amplify the NMR signal as close as possible to the coil in order to avoid losses or noise introduced by coaxial cables and connectors.

Moreover, for low matter quantities analysis, the amplitude of the NMR signal is very weak. Let's illustrate this from the experimental values of our surface coil (R_s =4 Ω) and our microcoil (R_s =1.3 Ω) for a measured volume of 1 mm^3 under a static field of 4.7 T and a bandwidth of 4 kHz [22]. The measured voltage densities of the signals (S) and noises (N) are S = 465 nV/√Hz and N=16 nV/√Hz for the surface coil and S = 2.3 µV/√Hz and N= 9 nV/√Hz for the micro coil (state the influence of the filling factor: η = sample's volume / coil's volume). In the case of a 0.1 mm^3 [8], the measured SNR with the micro coil is 80 and the estimated voltage density of the signal is 720 nV/√Hz.

The SNR of a micrometric sample is as poor as it is for most of the RF receivers [16]. That is the reason why it is interesting to look at the low noise amplification used in the RF receivers.

Any device, connector or transmission line produces an internal noise which is added to the noise at the input of the device. In terms of power spectral density per unit of frequency (V^2/Hz), the SNR at the output of a device with a voltage gain G_v is given by [23]:

$$SNR_{out} = \frac{G_v^2 \times \overline{V_{s,in}^2}}{G_v^2 \times \overline{V_{n,in}^2} + \overline{V_{n,dev}^2}}, \quad (3)$$

Indeed, the input signal and the input noise are amplified with the same factor G_v. The noise factor of a device is defined as the ratio between the SNR at the input of the device and the SNR at the output:

$$F = \frac{SNR_{in}}{SNR_{out}}, \quad (4)$$

Even if the noise factor induced by the LNA is very low (F ≈ 1.1 for the best technologies [24]), the SNR at the output of any device is lower than the SNR at its input (F > 1). But the importance of the LNA is illustrated by the Friis formula [17] which is the expression of the noise factor at the end of an impedance matched data acquisition line:

$$F = F_1 + \frac{F_2 - 1}{G_{v,1}^2} + \frac{F_3 - 1}{G_{v,1}^2 G_{v,2}^2} + \cdots \quad (5)$$

The interest of the LNA is to amplify the signal at the input of the data acquisition line (introducing the lower noise as possible) in order to improve the SNR at the output of the system. The higher the gain of the LNA is and the lower the noise added by the LNA is, the better the SNR at the output of the data acquisition line will be. And the closer the LNA is to the receiver coil, the lower the input noise produced by transmission lines will be.

The minimum noise factor of a device can also be represented by the equivalent noise temperature referred at the input of the system (T_{eq}, in K) and the noise temperature of the source (T_s, which is the ambient temperature in K):

$$F = 1 + \frac{T_{eq}}{T_S}, \quad (6)$$

2.2. Low Noise Matching Network Requirements for NMR Receiver Coils

The matching network is a passive devices network placed between the coil and the amplifier (or transmission line) where the aim is to deliver the output signal in the better conditions (voltage, power, frequency selection…) and also to avoid the reflection wave in the case of radio frequencies. In this part we will detail the requirements for an optimum low noise matching network for NMR receivers which involves the power matching, the voltage matching and the noise matching.

a) Power matching.

The classic matching network in NMR is based in the 50 Ω power matching as it is the characteristic impedance of most of the coaxial cables and terminals used in NMR. The interest of power matching in NMR is to avoid any reflection of the NMR signal from the circuit to the sample. Such a case can produce an error in the lecture of the relaxation times T1 and T2 and can also produce a perturbation of the homogeneity of the static magnetic field [25, 26].

Theoretically, if $\underline{Z_{coil}} = \underline{Z_{in}^*}$, the reflection wave will be zero, S11 will tend to -∞ dB and there will be a maximum power transfer (S21 = 0 dB); that is the raison why this is called the power matching. In practice, a 10 % reflection wave (S11 = -12 dB) is acceptable and that allows a mismatch range of +/-20 % between the impedance of the coil and the characteristic impedance of the transmission line.

b) Voltage matching

Considering R_s the equivalent resistance of the source and Z_{in} the impedance input of the LNA, the input noise is given by $\overline{V_{n,in}^2} = 4kTR_s$, the noise at the amplifier output is $\overline{V_{n,\text{out}}^2} = a^2 G_v^2 \overline{V_{n,\text{in}}^2} + \overline{V_{n\,amp}^2}$ and the output signal is $V_{\text{out}}^2 = a^2 G_v^2 V_{s,in}^2$ with the voltage ratio $a = Z_{in} / (Z_{in} + R_s)$. From Eq. 4, we can express the noise factor as follows:

$$F = \frac{a^2 G_v^2 \overline{V_{n,in}^2} + \overline{V_{namp}^2}}{a^2 G_v^2 \overline{V_{n,in}^2}} = 1 + \frac{\overline{V_{namp}^2}}{a^2 G_v^2 \overline{V_{n,in}^2}} \quad (7)$$

From this relation, we can state that for high input impedance compared to R_s, α = 1 and the second term of the noise figure will be minimized. With this condition we will have a maximum voltage transfer from the coil to the input amplifier ensuring the voltage matching. An example of application of the voltage matching to minimize the noise figure is given in [23].

c) Noise matching

To have a deep understand of the noise model of an amplifier we need to understand the noise theory of two port networks [27] and a transistor noise model [28].

A noisy two port network can be modeled as a noiseless two port network with an input noise voltage source ($\overline{V_n}$) and an input current noise source ($\overline{I_n}$) [29]. $\overline{V_n}$ is the equivalent voltage source referred to the input when the input is short-circuited ($Z_{sourse} = 0$) and $\overline{I_n}$ is the equivalent current source referred to the input when the input is open-circuited ($Y_{sourse} = 0$). These equivalent sources are correlated because they represent the global behavior of the internal physical noise sources of the noisy two ports.

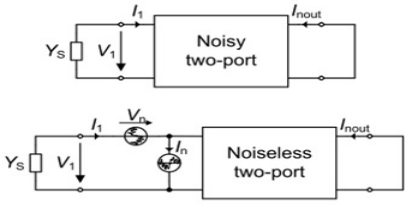

Fig. 2. Noisy-Two port model.

In amplifiers, the noise factor can be described by:

$$F = F_{\min} + \frac{g_n}{R_S}\left|Z_{source} - Z_{opt}\right|^2 = \\ = F_{\min} + \frac{g_n}{R_S}\left[\left(R_S - R_{opt}\right)^2 - \left(X_S - X_{opt}\right)^2\right] = \\ = F_{\min} + \frac{r_n}{G_S}\left[\left(G_S - G_{opt}\right)^2 - \left(B_S - B_{opt}\right)^2\right] \quad (8)$$

where F_{min} is the minimum noise factor of the amplifier, g_n is the noise conductance, $G_{source}=R_s+X_s$ is the impedance of the source and Z_{opt} is the optimum source impedance value that allow us to reach the minimum noise factor. Then the noise matching is achieved when $R_s=R_{opt}$ and $X_s=X_{opt}$. Respectively, r_n is the noise conductance, G_{source} is the admittance of the source and Y_{opt} is the optimum source admittance. The noise conductance, the noise resistance and their relationship are defined as follows [28, 30, 31]:

$$g_n = \overline{I_n^2}/(4k_B T), \quad (9)$$

$$r_n = \overline{V_n^2}/(4k_B T), \quad (10)$$

$$g_n R_{opt} = r_n G_{opt}, \quad (11)$$

The noise parameters to define are then: F_{min}, g_n (or r_n), R_{opt} (or G_{opt}) and X_{opt} (or B_{opt}) and they can be described as a function of the internal transconductance, capacitances and resistances of the two port network [29]. Usually, $Z_{in}\neq Z_{opt}$. A Low Noise Amplifier is then an amplifier where F_{min} and g_n (or r_n) are as low as possible.

3. Model of the Circuit and Simulations

In order to determine the optimum noise matching network by simulation performed by ADS® software, we need to have a model of the coil and the amplifier as reliable as possible around 200 MHz (^{1}H resonant frequency under 4.7 T field of NMR system).

3.1. Coil Model

An NMR receiver coil is a transducer that converts the instantaneous nuclear magnetization vector $\overrightarrow{M(t)}$ of a sample in a voltage free induction *decay* (FID). The signal processing of the measured FID gives the signal information that allows the reconstruction of the sample images or spectra.

From the energy conversion point of view, the variation of the magnetization vector produces a flux variation through the static NMR receiver coil. The magnetic induction is then placed in a Neumann case [32]. Under this condition, from the differential forms of the Gauss's law and the differential Maxwell-Faraday equation, we can show that the instantaneous electric field produced by the magnetization vector in a point m of the circuit of a coil is given by [33]:

$$\vec{E}_{(m,t)} = -\overrightarrow{grade}\,(V(t)) - \overrightarrow{\frac{\partial A_{(m,t)}}{\partial t}}, \quad (12)$$

In a quasi-stationary regime, the local Ohm's law in a point m of the circuit is:

$$\vec{J}_{(m,t)} = \sigma \vec{E}_{(m,t)}, \quad (13)$$

And the local resistance is:

$$d\vec{R} = \frac{d\vec{l}}{\sigma S}, \quad (14)$$

where σ is the conductivity of the circuit and S is its section. From the equation (12), the electric field in a portion AB of the coil is:

$$\int_A^B \vec{E}_{(m,t)} d\vec{l} = -(V_B(t) - V_A(t)) + \\ + \int_A^B \left(-\overrightarrow{\frac{\partial A_{(m,t)}}{\partial t}}\right) d\vec{l}, \quad (15)$$

From the equations (13) and (14):

$$\vec{E}_{(m.t)} d\vec{l} = \int_A^B \frac{\vec{j}_{(m,t)}}{\sigma} d\vec{l} = \int_A^B \frac{\vec{I}_{(m,t)}}{\sigma s} d\vec{l} = \\ \int_A^B \vec{I}_{(m,t)} d\vec{R} = R_{AB} I_{AB}(t), \quad (16)$$

Moreover, the induced electromotive force in the Neumann case is:

$$e_\Phi(t) = -\frac{d\Phi}{dt} = \int_A^B \left(-\overrightarrow{\frac{dA}{dt}_{(m,t)}}\right) d\vec{l}, \quad (17)$$

By combining the equations (15), (16) and (17), and considering AB the terminals of the coil, we deduce the potential difference of NMR receiver as:

$$V_{coil}(t) = V_B(t) - V_A(t) = e_\Phi(t) - R_{AB} I_{AB})(t) \quad (18)$$

From a transducer point of view, this expression means that the coil has a Thevenin equivalent circuit where e_ϕ is the voltage generator (induced by the flux variation) with an internal loss resistance R_{AB} (Fig. 3). The Norton equivalent circuit between the terminals AB of the coil is a current generator $i_\phi=e_{AB}/R_{AB}$ with an internal loss resistance R_{AB}.

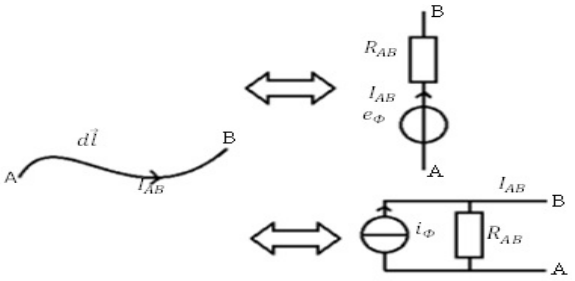

Fig. 3. Thevenin-Norton equivalent circuit of a coil from a transducer point of view.

From a frequency resonant point of view, we have to add the equivalent circuit the physical proper inductance between the terminals AB. The complete equivalent model of an NMR receiver coil is then a parallel RL circuit with an induced current source i_ϕ. This model contrasts with the series RL equivalent circuit, widely used in the NMR community.

In the Fig. 4, we plot the S11 parameter of the impedance Z_{AB} of an equivalent parallel RLC circuit and an equivalent series RLC circuit. For the same values of R, L and C, we clearly see that the series RLC circuit acts like a low pass filter and the parallel RLC circuit acts like a selective filter which is actually the real behavior of an NMR receiver coil.

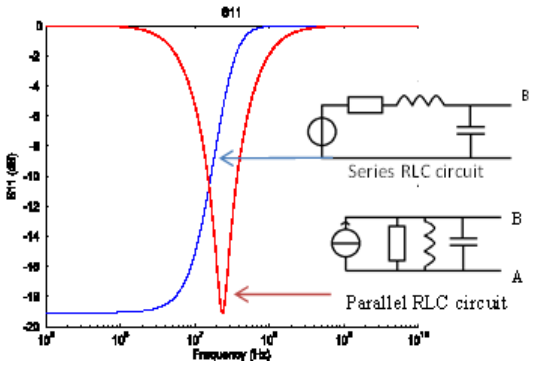

Fig. 4. RLC series and parallel S11 comparison.

Moreover, in an RL series circuit, the inductance L_{AB} is a loss element and this approach disagrees with the energy conversion demonstration where no inductance takes part (equation 18).

We conclude that an NMR receiver coil should be modeled by its equivalent Norton (or Thevenin) circuit in parallel whit the physical inductance L_{AB}.

3.2. Amplifier Model: Estimation of the Noise Parameters

To model the commercial amplifier, first we extract the S-parameters with a VNA (E5071C ENA series, Agilent Technologies). From the S11 parameter, we can get a model of the input impedance of the amplifier. The parameter S21 allows us to determine the power gain of the device. S12 (< -60 dB) states that the amplifier is unilateral, probably achieved with an output cascade stage. S22 give us information about the output impedance.

The stability of the amplifier can be checked by using the Rollett stability factors K and Δ [34].

$$\Delta = S_{11}S_{22} - S_{12}S_{21}, \tag{19}$$

$$K = \frac{1 - S_{11}^2 - S_{22}^2 + \Delta^2}{2\left|S_{12}S_{21}\right|}, \tag{20}$$

In this case K > 1 and Δ < 1; thus, our commercial amplifier is unconditionally stable for any passive load or source impedance.

Concerning the noise parameters, F_{min} is given in general by the constructor but often it is not the case for g_n and Z_{opt}. From the S-parameters of our amplifier we can assume that our LNA is based in an inductive series feedback design and the particularity of this design technique is that we can have a simultaneous power and noise matching which means that $Z_{in}=Z_{opt}$ [35], [36]. By taking this simplifying hypothesis, we can estimate g_n thanks to the inequality of Pospieszalski [30], [31]:

$$1 \le \frac{4R_{opt}\,g_n}{F_{\min} - 1} < 2, \tag{21}$$

The left side inequality means that the correlation between the input equivalent two noise sources may not be correlated more than 100 % the right side is a limitation of the model [31].

From the equation (6) and the Johnson-Nyquist formula [21] we find that:

$$F_{\min} - 1 = \overline{V_n I_n}/(2k_B T_S), \tag{22}$$

By combining the equations (9), (21) and (22) we can deduce (21) to (23).

$$\begin{cases} \dfrac{1}{2R_{opt}} \le \dfrac{\overline{I_n}}{\overline{V_n}} < \dfrac{1}{\mathrm{R_{opt}}} & (23) \\ \overline{V_n I_n} = (F_{\min} - 1)\times(2k_B T) & (24) \end{cases},$$

In order to estimate the equivalent input noise sources, we have to verify the system above.

From the constructor datasheet, the minimum noise figure is $NF_{\min} = 0.45\,dB$, thus the minimum noise factor is: $F_{\min} = 1.1092$.

For a work temperature of 293 K, we have: $\overline{V_n I_n} = 8.82 * 10^{-22}$ J/Hz. Thus, the estimated values of the equivalent input noise sources at 200 MHz are:

$$\overline{V_n} = 38\,pV/\sqrt{Hz}$$
$$\overline{I_n} = 23.2\,pA/\sqrt{Hz}$$

These values allow calculating g_n and r_n to complete the model of our commercial amplifier and we can create a file type ".s2p" to be used for the circuit simulations. The results here stay estimation but it is enough for a basic simulation. A more precise method to extract the noise sources values from measured data is presented by Ikalainen [37].

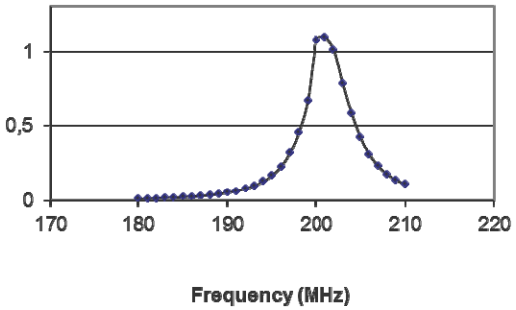

Fig. 5. Inequality of Pospieszalski plot for the estimated noise sources values.

3.3. Noise Matching Network Simulation

With a defined model of the coil and the amplifier, we can define the noise matching network between them (Fig. 6).

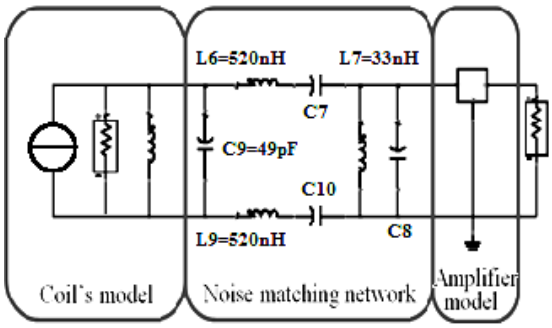

Fig. 6. Final circuit simulation.

The capacitor C9 is the tuning capacitor but in practice it also has an important matching influence. The inductance L6 mainly influence the tuning of the circuit and L7 varies the matching at the input of the amplifier. The capacitors C7 and C8 do not have a major impact on the circuit behavior and they are as low as possible (1 pF). L9 and C10 are the same as L6 and C7, this impedance repartition is used to compensate the dielectric losses [38].

The Fig. 7 shows the evolution of the AC voltage through the circuit. V_{in} is the input signal at the terminals of the coil (L8), V_a is the voltage at the amplifier's input and V_{out} is the output voltage. We can state that the maximum value of the input voltage is reached about 225 MHz; this value corresponds to the resonance between the inductance of the coil (L8) and C9. As we can see, the maximum voltage gain through the circuit is reached at about 210 MHz and not at the resonance frequency of the coil. This is because the voltage gain strongly depends on the matching network and mainly in the inductance L7 according to the voltage matching (equation 7).

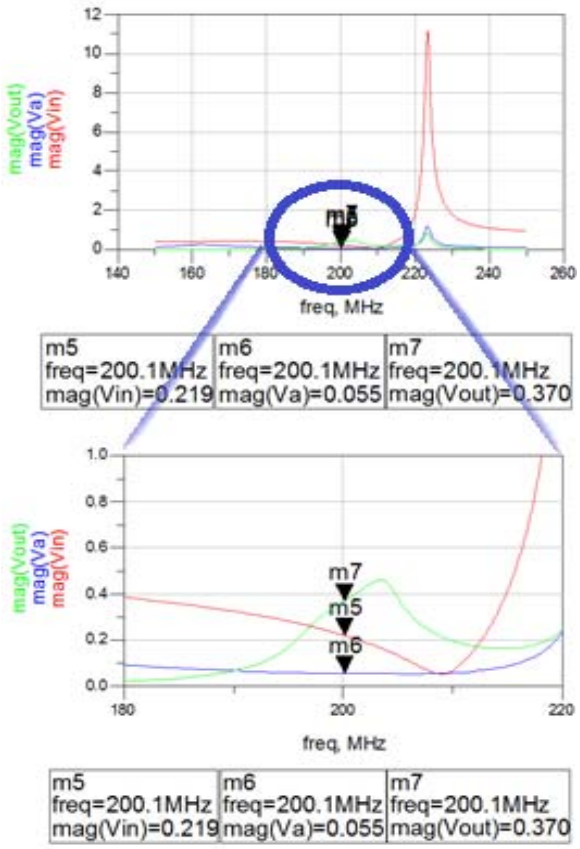

Fig. 7. AC voltage evolution.

The optimum matching network is accomplished when the combination of this capacitors and inductances allows obtaining the three low noise matching requirements. With the component values of the circuit of the Fig. 6 we reach the optimum noise matching network requirements at 200 MHz (Fig. 8):

S21 = 12 dB and G_v = 13.8 dB (V_{out}/V_{in} = 4.8), which is a good compromise between the power gain of the NMR signal and the voltage matching allowing to minimize the noise at the input of the amplifier.

NF = 0.8 dB, final noise contribution of the matching network and the LNA to the NMR signal.

S11 = - 9.5 dB, this value is higher than the expected -12 dB but in practice that can be improved.

We must notice that a better power matching implies a worst noise figure as predicted by the opposition between the power and voltage matching.

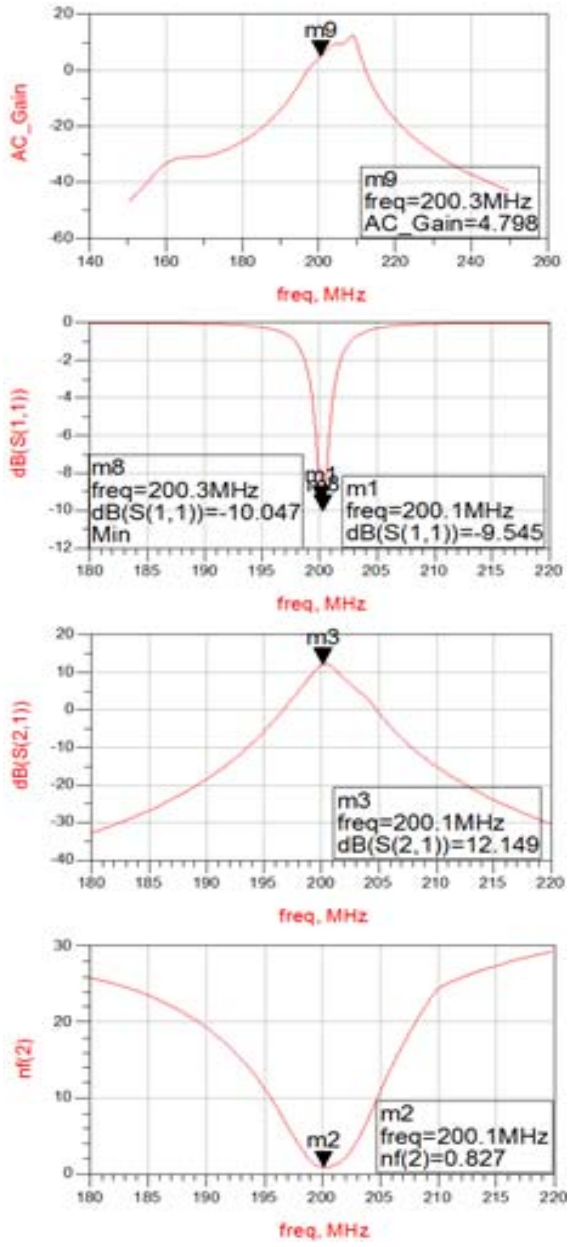

Fig. 8. Simulation results of the matching network requirements.

4. Results

The S-parameters of the circuit measured with the VNA match the results predicted by simulation and we validate the interest of the *in situ* LNA for NMR receivers.

The circuit is fabricated in an FR-4 PCB with a 35 µm copper thickness. The surface coil is a loop with radius of 1.5 cm. the coil is linked to the matching network and the amplifier by a strip line of 7.5 cm. In order to avoid any losses or noise introduced by switches of PIN diodes, behind the LNA, we have a GaAs based SPDT RF-switch that ensures the decoupling of the coil during the RF- excitation.

The achieved circuit is showed in the Fig. 9. The receiver coil and the electronic part are separated each other to avoid interaction between the emitting coil and the sample with the electromagnetic field emitted by the electronic circuit and also to avoid field inhomogeneity of the gradients due to the Faraday cage that encapsulates the circuit.

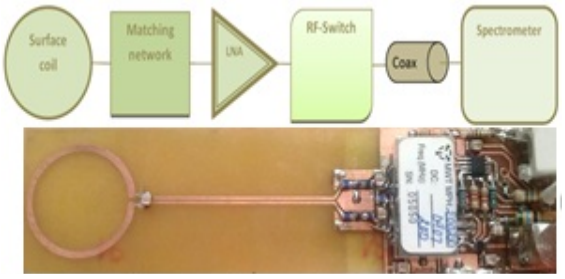

Fig. 9. Circuit stages and achieved in situ low noise amplified NMR coil.

4.1. Test Bench Verification

To verify the circuit model and the simulations based in the theory presented in this study we measure the S-parameters of the total final circuit with the VNA (E5071C ENA series, Agilent Technologies). In the Fig. 10, at 200 MHz, we can see that S11 = -12.5 dB and S21 = 9.4 dB match the simulation results as well as the measured voltage gain of 4.

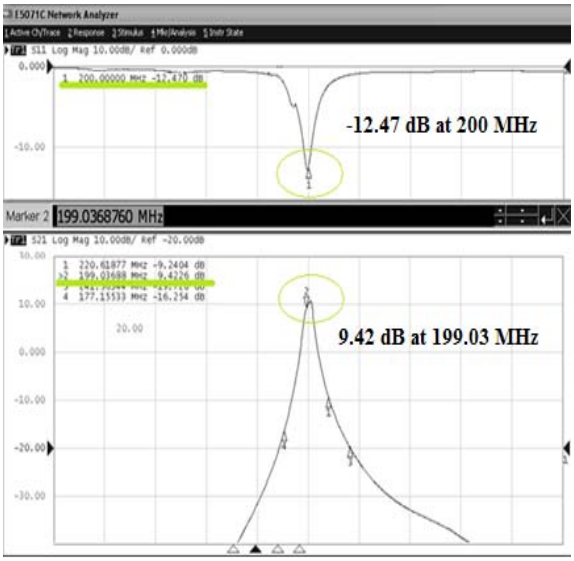

Fig. 10. Measured S11 (top) and S21 (bottom).

The similarity between the measured S-parameters and voltage gain and the simulation results allow us to conclude that the power and voltage matching are achieved. The measurement of the noise in the circuit requires a specific VNA that we does not have in our laboratory so we are not able to verify the noise matching. However, as the

measurements and simulation of the S-parameters and voltage gain are very close, we can assume that the noise matching is also achieved.

4.2. Practical Validation

To validate the influence of our circuit on the SNR, we made an MRI comparison between the circuit of the Fig. 9 and a classic 1.5 cm radius surface coil (surface coil, 50 Ω matching network and coaxial cable to the spectrometer). This comparison was based in a RARE sequence with 2 mm coronal slices (parallel to the surface of the coil) under a 4.7 T Bruker system.

The SNR is measured in slices parallel to the axial plan of the coil at a progressive distance. In the Fig. 11, we have a qualitative comparison of the SNR obtained for the same slice with the classic coil configuration and the *in situ* low noise amplified coil.

With the plot at the top of the Fig. 12, we can state that the SNR of the amplified coil is higher than 50 dB till a distance of 16 mm to the coil while the maximum SNR of the classic configuration is 31 dB for a distance of 4 mm. The LNA allow us to have a deeper field of view into the sample with a better SNR than the classic coil.

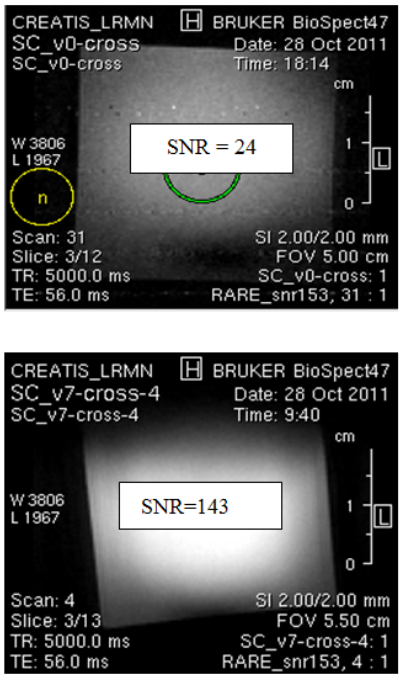

Fig. 11. Images obtained with a classic coil (top) and the in situ low noise amplified coil (bottom).

In the bottom of the Fig. 12 we have the mean SNR improvement which is the average ratio between the amplified coil and the classic coil. For a distance to the coil between 4 mm and 26 mm, we have a SNR improvement between 5 and 3. The in situ low noise amplification allows us to improve the sensitivity of the coil as far as 6 fold for a NMR measurement at 6 mm to the coil.

In terms of MRS, the concentration limit of detection is: $LOD_c = 3/S_c$. By applying this method to the microcoil, we will be able to detect a minimum choline concentration of 1.7 mM for a 100 mM concentration of cerebral metabolites solution. This is equivalent to a 6 % reduction of the in situ amplified microcoil LOD_c compared to the actual non amplified microcoil.

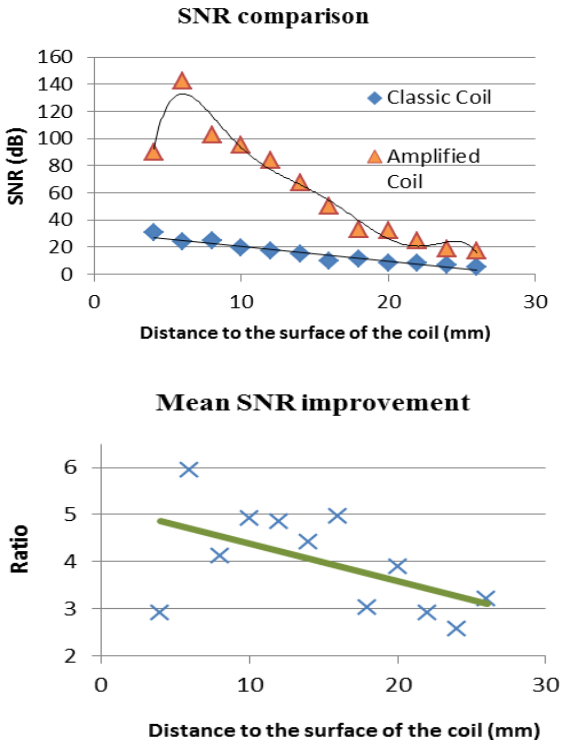

Fig. 12. SNR comparison between the classic coil and the local amplified coil (top) and the mean ratio of the SNR improvement of the amplified coil in comparison to the classic coil (down).

5. Conclusions

The NMR receiver coils are critically important in performance of NMR imaging and spectroscopy system. In this work we showed the interest of an in situ low noise amplification applied to NMR receiver coils. Here we detailed the requirements to reach an optimized matching network allowing simultaneously a suitable voltage gain, noise figure and S-parameters. In addition, an optimum transmission of the signal from the coil to the amplifier is obtained by avoiding the use of coaxial cables and switches between the coil and the LNA. In order to have reliable simulation results, we proposed a novel approach to define a model of an NMR receiver coil representing its real behavior and we also proposed a method to estimate the noise conductance and noise resistance of an inductive series feedback LNA.

We also showed that the achievement of the low noise matching network requirements in NMR allows having a factor 6 sensitivity improvement of a given coil. This method allows having a 4 fold deeper field of view in MRI and can be applied to NMR coil and microcoils to obtain a lower concentration limit of detection in MRS.

Thus, this study is contribution toward obtaining better acquisitions with NMR receiver coils and most particularly with micro receiver coils.

References

[1]. F. V. Gilroy, M. R. Edwards, R. S. Norton, & W. J. O'Sullivan, Metabolic studies of the protozoan parasite, Crithidia luciliae, using proton nuclear magnetic resonance spectroscopy, *Mol. Biochem. Parasitol*, Vol. 31, Issue 2, 1988, pp. 107-115.

[2]. J. K. Nicholson, P. J. D. Foxall, M. Spraul, R. D. Farrant, & J. C. Lindon. 750 MHz 1 H and 1 H-13C NMR Spectroscopy of Human Blood Plasma, *Analytical Chemistry*, Vol. 67, Issue 5, 1995, pp. 793-811.

[3]. R. Teng, P. R. Junankar, W. A. Bubb, C. Rae, P. Mercier, & K. Kirk, Metabolite profiling of the intraerythrocytic malaria parasite Plasmodium falciparum by 1 H NMR spectroscopy, *NMR in Biomedicine*, Vol. 22, Issue 3, 2009, pp. 292-302.

[4]. R. Subramanian, M. M. Lam, & A. G. Webb, RF microcoil design for practical NMR of mass-limited samples, *Journal of Magnetic Resonance*, Vol. 133, Issue 1, 1998, pp. 227-231.

[5]. P. J. M. van Bentum, J. W. G. Janssen, & P. M. Kentgens, Towards nuclear magnetic resonance μ-spectroscopy and μ-imaging, *Analyst*, Vol. 129, 2004, pp. 793-803.

[6]. C. Massin, F. Vincent, A. Homsy, K. Ehrmann, G. Boero, P.-A. Besse, A. Daridon, E. Verpoorte, N. F. de Rooij, & R. S. Popovic, Planar microcoil-based microfluidic NMR probes, *Journal of Magnetic Resonance*, Vol. 164, Issue 2, 2003, pp. 242-255.

[7]. N. Baxan, J. F. Chateaux, A. Rengle, H. Rabenson, A. Briguet, G. Pasquet, P. Morin, & L. Fakri-Bouchet, NMR implantable probe: limit of metabolites detection. in *ISMRM,* in *Proceedings of the 17th Annual Workshop on Circuits, Systems and Signal Processing*, Veldhoven, The Netherlands, 2006, pp. 125-131.

[8]. N. Baxan, H. Rabeson, G. Pasquet, J.-F. Châteaux, A. Briguet, P. Morin, D. Graveron-Demilly, L. Fakri-Bouchet, Limit of detection of cerebral metabolites by localized NMR spectroscopy using microcoils, *Comuptes Rendus Chimie*, Vol. 11, 2008, pp. 448-456.

[9]. A. Kadjo, N. Baxan, R. Cespuglio, C. Rousset, A. Briguet, D. Graveron-Demilly, L. Fakri-Bouchet, In vivo animal NMR studies using implantable micro coil, in *IEEE Imaging Systems and Techniques*, 2008, pp. 294-296.

[10]. A. Kadjo, N. Baxan, R. Cespuglio, A. Briguet, C. Rousset, M. Dung-Hoang, D. Graveron-Demilly, & L. Fakri-Bouchet, In vivo animal NMR studies using implantable micro-coil, in *Proceedings of the ISMRM, 17th Scientific Meeting and Exhibition*, Honolulu, USA, 2009, pp. 4275.

[11]. A. Kadjo, J. C. Brisset, M. Dung-Hoang, P. Poulichet, C. Rousset, A. Fakri, Y. Z. Wadghiri, M. Wiart, L. Rousseau, R. Cespuglio, A. Briguet, D. Graveron-Demilly, & L. Fakri-Bouchet. Biocompatibility of implantable micro-coil dedicated for In vivo animal NMR studies. in *ISMRM,* in *Proceedings of the 18th Scientific Meeting and Exhibition*, Stokholm, Sweden, 2010.

[12]. L. Fakri-Bouchet, T. Cherifi, L. Quiquerez, J. F. Chateaux, & A. Briguet, High performance NMR local preamplifier associated to microcoil, in *Proceedings of the 13th Scientific Meeting and Exhibition (ISMRM)*, Miami Beach Florida, USA, 2005, pp. 409.

[13]. K. R. Minard & R. A. Wind, Solenoidal microcoil design - Part II: Optimizing winding parameters for maximum signal-to-noise performance, *Concepts in Magnetic Resonance*, Vol. 13, 2001, pp. 190-210.

[14]. S. J. Dodd, G. C. Nascimiento, M.-C. Hsieh, H. Merkle, J. A. Murphy-Boesch, J. H. Chen, A. P. Koretsky, & A. C. Silva, Modular Preamplifier Design and Application to Animal Imaging at 7 and 11.7 T, in *Proceedings International Society for Magnetic Resonance in Medicine*, 2009, p. 2985.

[15]. R. P. Joensuu, Array RF Coil for Rabbit Thoracic Arteries Imaging at 200MHz, in *Proceedings of the International Society for Magnetic Resonance in Medicine*, 2009, p. 4736.

[16]. F. Bruccoleri, E. A. M. Klumperink, & B. Nauta, Wideband Low Noise Amplifiers Exploiting Thermal Noise Cancellation, *Kluwer/Springer*, Dordrecht, Netherlands, 2005.

[17]. H. T. Friis, Noise Figures of Radio Receivers, in *Proceedings of the IRE*, Vol. 32, Issue 7, 1944, pp. 419-422.

[18]. M. E. Lacey, R. Subramanian, D. L. Olson, A. G. Webb, & J. V. Sweedler, High-Resolution NMR Spectroscopy of Sample Volumes from 1 nL to 10 μL, *Chemical Reviews*, 99, 1999, pp. 3133-3152.

[19]. R. R. Ernst, Application of Fourier Transform Spectroscopy to Magnetic Resonance, *Review of Scientific Instruments*, Vol. 37, Issue 1, 1966, pp. 93.

[20]. E. Harel, Magnetic resonance detection: spectroscopy and imaging of lab-on-a-chip, *Lab on a Chip*, Vol. 9, Issue 1, 2009, p. 17.

[21]. H. Nyquist, Thermal Agitation of Electric Charge in Conductors, *Physical Review*, Vol. 32, Issue 1, 1928, pp. 110-113.

[22]. A. Kadjo, Micro-capteur implantables: Etude des critères de performance en vue de l'optimisation des acquisitions par Spectroscopie RMN in vivo. Ph.D. Thesis, *Universite Claude Bernard Lyon1*, Lyon, France, 2011.

[23]. N. Sun, Y. Liu, H. Lee, R. Weissleder, & D. Ham, CMOS RF biosensor utilizing nuclear magnetic resonance, *IEEE J. Solid-State Circuits*, Vol. 44, 12, 2009, pp. 3677-3726.

[24]. NEC. NE67300 Low Noise Ku-K band GaAs MESFET, *Datasheet*, 2013.

[25]. D. H. Wu, A. Chen, & C. S. Johnson, Flow Imaging by Means of 1D Pulsed-Field-Gradient NMR with Application to Electroosmotic Flow, *Journal of Magnetic Resonance*, Series A, Vol. 115, 1995, pp. 123-126.

[26]. H. Barjat, D. L. Mattiello, & R. Freeman, Suppression of Radiation Damping in High-

Resolution NMR, *Journal of Magnetic Resonance*, Vol. 136, 1999, pp. 114-117.
[27]. H. Rothe & W. Dahlke, Theory of Noisy Fourpoles, in *Proceedings of the IRE*, Vol. 44, 1956, pp. 811-818.
[28]. A. Cappy, Noise modeling and measurement techniques (HEMTs), *IEEE Transactions on Microwave Theory and Techniques*, Vol. 36, 1988, pp. 1-10.
[29]. C. Enz & Y. Cheng, MOS transistor modeling for RF IC design, *IEEE Journal of Solid-State Circuits*, Vol. 35, 2000, pp. 186-201.
[30]. M. W. Pospieszalski, Modeling of noise parameters of MESFETs and MODFETs and their frequency and temperature dependence, *IEEE Transactions on Microwave Theory and Techniques*, Vol. 37, 1989, pp. 1340-1350.
[31]. M. W. Pospieszalski, On the Measurement of Noise Parameters of Microwave Two-Ports, *IEEE Transactions on Microwave Theory and Techniques*, Vol. 34, 1986, pp. 456-458.
[32]. P. Graneau, The Ampere-Neumann Electrodynamics of Metallic Conductors, *Fortschritte der Physik*, Vol. 34, 1986, pp. 457-501.
[33]. D. Fleisch, A Student's Guide to Maxwell's Equations, *Cambridge University Press*, 2008.
[34]. J. Rollett, Stability and Power-Gain Invariants of Linear Twoports, *IRE Transactions on Circuit Theory*, Vol. 9, 1962, pp. 29-32.
[35]. D. D. Henkes, LNA Design Uses Series Feedback to Achieve Simultaneous Low Input VSWR and Low Noise, *Applied Microwaves & Wireless*, 1998, pp. 26-32.
[36]. Z. Nie, J. Bao, P. Lin, & F. Cai, A novel simultaneous noise and input VSWR matching technique for broadband LNA, *Journal of Electronics (China)*, Vol. 27, 2011, pp. 446-452.
[37]. P. K. Ikalainen, Extraction of device noise sources from measured data using circuit simulator software, *IEEE Transactions on Microwave Theory and Techniques*, Vol. 41, 1993, pp. 340-343.
[38]. M. Decorps, P. Blondet, H. Reutenauer, J. Albrand, & C. Remy, An inductively coupled, series-tuned NMR probe, *Journal of Magnetic Resonance*, Vol. 65, 1985, pp. 100-109.